

## NRC Publications Archive Archives des publications du CNRC

### Freezing of water in portland cement paste: an a.c. impedance spectroscopy study

Perron, S.; Beaudoin, J. J.

This publication could be one of several versions: author's original, accepted manuscript or the publisher's version. / La version de cette publication peut être l'une des suivantes : la version prépublication de l'auteur, la version acceptée du manuscrit ou la version de l'éditeur.

For the publisher's version, please access the DOI link below. / Pour consulter la version de l'éditeur, utilisez le lien DOI ci-dessous.

#### **Publisher's version / Version de l'éditeur:**

[https://doi.org/10.1016/S0958-9465\(01\)00078-6](https://doi.org/10.1016/S0958-9465(01)00078-6)

*Cement and Concrete Composites - Special Edition on Application of Electrical Methods*, 24, pp. 467-475, 2002-09-01

#### **NRC Publications Archive Record / Notice des Archives des publications du CNRC :**

<https://nrc-publications.canada.ca/eng/view/object/?id=14fc4dea-ce37-4640-833d-9ca2929806f6>

<https://publications-cnrc.canada.ca/fra/voir/objet/?id=14fc4dea-ce37-4640-833d-9ca2929806f6>

Access and use of this website and the material on it are subject to the Terms and Conditions set forth at

<https://nrc-publications.canada.ca/eng/copyright>

READ THESE TERMS AND CONDITIONS CAREFULLY BEFORE USING THIS WEBSITE.

L'accès à ce site Web et l'utilisation de son contenu sont assujettis aux conditions présentées dans le site

<https://publications-cnrc.canada.ca/fra/droits>

LISEZ CES CONDITIONS ATTENTIVEMENT AVANT D'UTILISER CE SITE WEB.

**Questions?** Contact the NRC Publications Archive team at

PublicationsArchive-ArchivesPublications@nrc-cnrc.gc.ca. If you wish to email the authors directly, please see the first page of the publication for their contact information.

**Vous avez des questions?** Nous pouvons vous aider. Pour communiquer directement avec un auteur, consultez la première page de la revue dans laquelle son article a été publié afin de trouver ses coordonnées. Si vous n'arrivez pas à les repérer, communiquez avec nous à PublicationsArchive-ArchivesPublications@nrc-cnrc.gc.ca.



# **NRC - CNRC**

## **Freezing of water in portland cement paste - an ac impedance spectroscopy study**

**Perron, S.; Beaudoin, J.J.**

**NRCC-44492**

A version of this document is published in / Une version de ce document se trouve dans :  
Cement and Concrete Composites, v. 24, 2002, pp. 467-475

[www.nrc.ca/irc/ircpubs](http://www.nrc.ca/irc/ircpubs)

# **FREEZING OF WATER IN PORTLAND CEMENT PASTE – AN A.C. IMPEDANCE SPECTROSCOPY STUDY**

S. Perron\* and J.J. Beaudoin\*\*+

\*Department of Civil Engineering University of Ottawa,  
Ottawa Canada, K1N 6N5

\*\* Institute for Research in Construction, National Research Council,  
Ottawa Canada, K1R 0R6

## **ABSTRACT**

The freezing of water in Portland cement paste was investigated using a.c. impedance spectroscopy techniques. Length change and impedance measurements on cooling and warming were obtained simultaneously using a specially designed coupling technique. A new descriptor of frost resistance is described in terms of the high frequency arc depression angle in the impedance plane. Curves of the depression angle parameter  $\phi$  versus temperature are shown to be indicative of the pore structure and its effect on mass transfer of water and nucleation and growth of ice crystals. The  $\phi$  - temperature and resistance-temperature curves are used in combination to assess structural damage. Results are compared with those obtained for model pore systems i.e. vycor glass and clay brick.

Keywords: freezing, cement paste, impedance, depression angle.

+ Corresponding author

# **Freezing of Water in Portland Cement Paste-an A.C. Impedance Spectroscopy Study**

## **INTRODUCTION**

Saturated porous solids including Portland cement binders can suffer mechanical damage in non-equilibrium freezing-thawing cycles [1]. Rapid cooling results in significant temperature and moisture gradients and considerable stress. Inhomogeneity created by rapid wetting and drying is known to create stresses that result in cracking. The very high rate of drying during cooling to temperatures below 0°C contributes significantly to damage due to frost action.

The general problem of damage caused by freezing in various porous materials has been the subject of much study [2-4]. Common aspects of the freezing phenomenon have been identified. Attempts have also been made to describe freezing processes by a thermodynamic approach [5-7]. These describe the freezing process in terms of the mass transfer of water and nucleation and growth of ice crystals in pores [ 7]. There remains some debate as to whether mass transport of water alone (on cooling) can cause damage.

The test methods for assessing the frost resistance of cement-based materials are varied and well described in the literature [ 8]. Volume change, mass change or change in dynamic modulus of concrete are often used as descriptors of durability. These characteristics are of significant practical value but do not necessarily provide direct evidence for a particular mechanism of frost action. Recently electrical methods have been used to study the freezing- thawing process [9-10]. They are particularly sensitive to nucleation and growth of ice crystals. Decreases in d.c. conductivity and low frequency dielectric constant values of two orders of magnitude have been observed at the initial freezing point of the aqueous solution in the macropores and larger capillary pores.

The authors have developed a method described below for simultaneous measurement of length change (from thermal mechanical analysis) and impedance characteristics of cement paste on cooling and warming. A feature of the impedance spectra, the frequency dispersion (or depression) angle was found to contain information on pore structure effects as they relate to mass transfer of unfrozen water, pore blocking, nucleation of ice crystals and pore filling with ice.

The ultimate goal of this work is to provide information useful for the development of a frost resistance test based on electrical measurement methods. The immediate objective is to understand the significance of the depression angle-temperature and resistance-temperature profiles on cooling and warming cement paste in the temperature range of ambient to -80°C.

## A.C. IMPEDANCE SPECTROSCOPY

The basic principles of a. c. impedance spectroscopy are described in detail elsewhere [11-13]. A brief description of the relevant aspects related to cement science will be given. An idealized impedance spectrum for a cement system is plotted in the real versus imaginary plane (Figure 1(a)). A single arc in the high frequency range with a small part of a second arc in a relatively low-frequency range is shown. The high-frequency arc (HFA) is attributed to the bulk paste impedance behavior. The second arc is due to the cement paste electrode interface surface capacitance contribution. The intercepts  $R_1$  (at the high frequency end) and  $R_1+R_2$  (at the minimum between the electrode arc and bulk arc) are important parameters providing information related to cement paste microstructure (e.g. porosity, pore size, ionic concentration of the pore solution) [14]. Interpretation of an impedance spectrum is usually based on modeling with an equivalent circuit (Figure 1(b)) until the electrical response of the elemental microstructure of the cement paste is well simulated.

In practice, an ideal semi-circle is generally not observed for most materials. It is normally an inclined semi-circle with its centre depressed below the real axis. This behavior, normally associated with a spread of relaxation times, cannot be described by the classical Debye equation employing a single relaxation time. A dispersive, frequency-dependent element or so-called constant phase element (CPE) can be introduced to account for the shape of the depressed complex plot [15]. The impedance contribution of this element can be expressed as follows:  $Z(\text{CPE})=A_0^{-1}(j\omega)^{-\alpha}$  where  $\alpha=1-2/\pi(\alpha)$  and  $\alpha$  is the depression angle.

Therefore,  $\alpha$ , can be used to represent the degree of perfection of the capacitor and represents a measure of how far the arc is depressed below the real impedance axis.

Previous work (by one of the authors) indicates a dependence of  $\alpha$  on the characteristics of the material pore size distribution [16]. Analysis of impedance spectra for cement paste, paste containing 5% silica fume and porous glass resulted in values of  $\alpha=0.68, 0.81$  and  $0.90$  respectively. The time for the orientation of ions or relaxation time appears to be affected by the geometry of the pores and the surface chemistry of the solid. It was suggested that a broad pore size distribution would result in a wide spread of relaxation times corresponding to a large dispersion angle. A narrow pore size distribution would result in a significantly reduced spread of relaxation times. The range of pore size distributions represented by the pastes and porous glass conforms to these arguments.

## EXPERIMENTAL

### Sample Preparation-Cement Paste

The cement paste test specimens were designed so that ACIS measurements as well as length change measurements could be taken simultaneously. Cement paste specimens were cast in 8 mm diameter cylinders, 13 mm long. The small cylinder size was selected to minimize gradients and to fit into the DuPont TMA apparatus. Stainless steel electrodes were cast in place at either end of the sample with approximately 2 mm cover. Silver wires were soldered onto the electrodes and used to connect the specimen to the Solartron 1260.

The stainless steel electrodes were held in place during placement of the cement paste by notching out the ends of the cylinder mould and securing the electrode in place with hot wax. The cement paste was placed into the mould in two steps. After each step the specimen was tamped several times to bring any air bubbles to the surface. The top electrode was then placed and secured with hot wax and a cover. Specimens with  $w/c=0.60$  were hydrated by rotating moulds for the first 24 hours to minimize bleeding.

The specimens were demolded the day following casting. They were wet cured in saturated calcium hydroxide solution for the desired hydration period. The pastes were made with  $w/c=0.35$  and  $0.60$ .

### Sample Preparation-Vycor Glass and Clay Brick

The specimens were of similar geometry to the cement paste specimens. The stainless steel electrodes were however attached to the ends of the cylindrical specimens using a conductive adhesive. The vycor glass had a surface area (determined by  $N_2$  absorption) of about  $100 \text{ m}^2/\text{g}$ . The mean pore size was 2.5 mm. The pore size distribution of the brick is plotted in Figure 2.

### Apparatus

The equipment used to measure the A.C. Impedance Spectroscopy (ACIS) response of the samples was the 1260 Solartron Gain-Phase Analyser. This apparatus was controlled by the computer software Z60.

The DuPont Thermo Mechanical Analyzer 2940 (TMA) apparatus was used to control the temperature variations as well as measure the changes in length of the specimen. Length change was measured through the movement of the probe. Liquid nitrogen was kept in the cold finger that lowered to enclose the specimen. The apparatus is equipped with a furnace to control the temperature variations at the desired rates.

The apparatus used to conduct the DSC and TGA tests were the DuPont 2910 and 951 analysers respectively.

### Testing Procedure

The test specimens were inserted into the DuPont TMA apparatus in a saturated surface dry condition. The wires connected to the electrodes were carefully placed so that they would extend outside the cold finger and yet would not interfere with it.

The following outlines the temperature regime used for each test:

1. Isothermal conditions at +5°C were held for 10 minutes. Impedance measurements were started at the beginning of the isothermal segment.
2. The temperature was decreased at a rate of 2°C/minute to a minimum of -80°C.
3. Isothermal conditions at -80°C were held for 10 minutes.
4. The temperature was increased at the rate of 2°C/minute to a maximum of +20°C
5. Isothermal conditions at +20°C were held for 5 minutes.

Each test was 114.5 minutes in duration. Several measurements of length were taken per minute and one impedance spectrum was stored every 50 seconds.

The raw data collected by Solarton 1260 Gain-Phase Analyzer was then fit to an equivalent circuit using the Zview software. Each impedance spectrum was fit to a corresponding equivalent circuit from which the sample resistance and dispersion angle parameter were obtained. For each test more than 130 impedance spectra were recorded and their corresponding equivalent circuits determined.

### Resaturation with Salt Solutions and Synthetic Pore Solution

In order to facilitate the resaturation of the cement paste samples (e.g. those containing salt solutions), the specimens were dried for 24 hours at 38°C, placed under a vacuum for three hours and then covered in the resaturation solution for eighteen hours while still under vacuum. This process will alter the pore structure of the cement paste. Therefore, in addition to resaturating the samples with salt solutions, similar samples were resaturated with a synthetic pore solution. To prepare the latter solution, saturated calcium hydroxide solution was used as a base and potassium chloride was added until the mixture produced the same resistance as natural pore water,  $\rho = 50 \text{ } \Omega \cdot \text{cm}$ . The effects of the salt solution on the behaviour of specimens during a freezing and thawing cycle were then compared to the specimens resaturated with the synthetic pore solution. Clay brick and vycor glass samples were also saturated with synthetic pore solution prior to testing.

## RESULTS AND DISCUSSION

The focus of this paper is on the electrical measurements. TMA results will only be briefly discussed. Changes to the overall sample resistance and the depression angle parameter ( $\theta$ ) of the high frequency arc are of specific interest. It is the combination of the resistance and  $\theta$  parameters that may provide new insights on the freezing process. These however are discussed independently and then in combination.

### 1. Sample Resistance

The sensitivity of impedance spectroscopy (ACIS) and the corresponding spectra (idealized in Figure 1) to changes in temperature can provide detailed information about the changes in the cement paste microstructure. Changes in the impedance spectra are extremely sensitive to freezing phenomena. For example the rapid growth of the high frequency arc in the complex plane (Figure 3) is initiated at the point of incipient freezing and the rate of growth during freezing is significant. It was anticipated that values of (ACIS) parameters would correlate with the amount of water freezing and the average pore size in which it freezes. The degree of hysteresis in the spectra would be indicative of pore structure damage.

The change of resistance ( $R_1+R_2$ , on the impedance plot) with temperature (for cement paste w/c=0.35, 1 day) is best described with reference to the plot in Figure 4. In the first section of the curve the increased resistance is occurring due to the reduced conductivity of the pore solution and the movement of the pore water. The first change in the slope of the resistance-temperature curve indicates that freezing has begun. Any subsequent change of slope indicates either primary freezing is no longer occurring or that secondary freezing is occurring. In general the incipient freezing temperatures (coincident with the first change in slope) decrease with increased hydration. This is compatible with the finer pore size distribution that is a result of continued hydration.

The less hydrated samples go through a longer range of resistance values on freezing. For the sample hydrated one day the slope of the resistance-temperature curve is the steepest and most distinctive. The slope changes of the 28 days specimens are not as pronounced as there is less pore water in each sample that freezes. The resistance continues to increase rapidly while there is still pore water freezing. Then the resistance continues to increase at a decreased rate due solely to a decrease in temperature.

A term, the effective freezing resistance (EFR) was defined as,  $R_{-40} - R_{if}/R_{if}$  and calculated for all specimens tested.  $R_{-40}$  and  $R_{if}$  are the resistance values at  $-40^\circ\text{C}$  and the incipient freezing temperatures respectively. This relative change in resistance, as expected, decreased with increased hydration and the concomitant decrease in the amount of water available to freeze, Table 1. The relationship between EFR and the amount of freezable water (as expressed by the integral of the heat flow curve, DSC analysis) is linear (Figure 5 (a)). This influence of the



amount of freezable water is clearly seen in a plot of  $R/R_0$  ( $R_0$  is the initial resistance) versus temperature (Figure 5 (b)). The normalized resistance is clearly much higher at early times of hydration.

## 2. Impedance Spectroscopy and the Depression Angle Parameter $\alpha$

### i) The $\alpha$ -Temperature ( $\alpha$ -T) curve

The phenomenon of the depressed arc on the impedance plot, as previously indicated, can be approximated using a constant phase element in the equivalent circuit. The depression angle of the high frequency arc is represented by  $\alpha$  in the equivalent circuit and they have an inverse relationship. The greater the degree of inhomogeneity of the sample (e.g. a porous system with a pore size distribution spanning a very wide range of pore sizes) the larger is the value of the depression angle, and therefore the smaller the value of  $\alpha$  (much less than 1). A  $\alpha$  value of 1 is indicative of a perfectly uniform (approached by a system with a very narrow range of pore sizes) pore structure. The freezing-thawing results in this investigation clearly show distinct relationships between  $\alpha$  and temperature.

Pore structure and surface inhomogeneity of the cement paste change with temperature and produce 'dynamic' changes in  $\alpha$ . Freezing results in the progressive filling of pores with solid ice (hence a dynamic change in pore structure) and the modification of the properties of surface absorbed layers of water (contributing to surface inhomogeneity).

A typical  $\alpha$  -temperature curve (Paste w/c=0.6, 1 day) is shown in Figure 6. A resistance-temperature curve is superimposed on the figure. It is apparent that  $\alpha$  is affected by the changes occurring within the pore system on freezing. The initial decrease in the value of  $\alpha$  with a decrease in temperature coincides with the occurrence of two phenomena i.e. some nucleation and formation of ice (where the temperature is below the triple point) and the movement of water. The movement of water increases as the temperature decreases below the triple point (due to free energy differences between super cooled liquid and bulk liquid) [5]. This has a dominant influence on the value of  $\alpha$ . Greater movement of water is analogous to movement through a more open pore structure (with a broader distribution of pores) in a paste system subjected to an externally applied pressure gradient. This is true even though the pore volume is actually reduced (to a limited degree) as ice begins to nucleate. The value of  $\alpha$  reaches a minimum when nucleation and growth of ice crystals is sufficient to block the pore space. This temperature is referred to as the pore blocking temperature. The movement of the pore water and freezing is increasingly affected by surface inhomogeneity and pore blocking resulting subsequently in a larger value of  $\alpha$ .

The minimum value of  $\rho$  is related to a significant amount of ice formation that fills entire pores and blocks electrical pathways. A direct consequence is a narrowing of the distribution of the remaining pores.

Since ice forms first in the larger pores, the effect of the ice formation is to reduce the effective size of the pore size distribution. The pore water has less mobility as a result of the blocked passageways. The combined effect is to increase the value of  $\rho$ .

The blocking temperature (corresponding to  $\rho_{\min}$ ) does not necessarily coincide with the point of incipient freezing previously defined in terms of the resistance parameter. The  $\rho$  value will continue to increase as the temperature is lowered below the pore blocking temperature. Virtually all the pore water capable of freezing has frozen at  $-40^{\circ}\text{C}$  and lower. However the value of  $\rho$  continues to increase. This could be due to the structure of the pore water in the micropores or absorbed water on surfaces that becomes more "ordered" with a decrease in temperature. A phase transition (water) is known to occur at  $-90^{\circ}\text{C}$ . The effect of pore surface roughness on electrical current paths may be modified.

(ii) Types of  $\rho$ -T Curves

The effect of pore size distribution variation in the test specimens is evident in the variety of  $\rho$ -T curves obtained (prevalent in the results for cement paste systems). There are four different types of  $\rho$ -T curves that reflect different pore structures. The curves are defined by the change in  $\rho$  before blocking occurs, the temperature range of the blocking temperature and the shape of the curve at minimum  $\rho$ . The four different types of curves (freezing-thawing) are illustrated in Figure 7. The first curve has a large change of  $\rho$  before blockage and no significant change of slope until the pore blocking temperature due to the freezing process. This implies a large pore size distribution that is well connected. Incipient freezing and blockage of the pores occur at similar temperatures. Type two, is defined by a small change of  $\rho$  before blocking and an early blocking temperature. This curve suggests a discontinuous system of large pores and has implications when freezing occurs in the presence of salt solutions due to the early blockage. The shape of the third curve indicates a large, broad pore size distribution. It has a large change in  $\rho$  before pore blockage and changes slope on freezing. The pore blocking temperature is low. Pastes with air entrainment usually follow this shape. Contrasting the deep valleys mentioned in the curves above, the fourth curve is shallow with a small change in  $\rho$  before blocking and has a flat section before climbing upwards. This curve implies a uniform pore structure that results in older pastes due to the additional hydration. The pore blocking temperature is usually low.

(iii) Air Entrainment and the  $\phi$ -T Curve

Further discussion regarding the effect of air-entrainment would appear warranted. Cement paste with air entrainment typically performs better during freezing and thawing than paste without air-entrainment [2]. The additional air bubbles in the paste provide locations where the supercooled pore water can find relief. The spacing of the entrained air is therefore important. If it is too great, the paste will be damaged before the pore water reaches the void.

The air-entrainment had a significant effect on the ACIS response of the paste on freezing and thawing. The pore blocking temperatures are quite low and the change in  $\phi$  before pore blockage is quite large. This indicates that there is significant movement of the pore water on freezing and that the additional porosity of the air-entrainment is being utilized.

The  $\phi$ -temperature curves with air-entrainment differ from the curves of the non-air-entrained samples by having a range of  $\phi$  leading to the pore blocking temperature equal to or greater than  $\phi_p$  between pore blocking and  $-80^\circ\text{C}$ . The initial values for R and  $\phi$  indicate that the entrained air is connected to the pore system. This leads to the lower initial values of R and high initial values of  $\phi$ . The extra porosity decreases R and the uniform pore size of the entrained air leads to a  $\phi$  value close to unity.

At  $-80^\circ\text{C}$ ,  $\phi$  does not approach one. This could mean that there is pore water left unfrozen at a range of pore sizes. Large hysteresis exists between freezing and thawing curves, for the  $\phi$ -temperature curve, about  $15^\circ\text{C}$ .

The resistance-temperature response of the air-entrained samples has a relatively gentle slope. The effective freezing resistance values of the  $w/c=0.35$  samples are low, being 9 at 7 days hydration and 7 at 28 days hydration (see Table 1). This indicates that the amount of pore water freezing is low.

For hydration of 28 days, the  $\phi$ -temperature curve on thawing does not follow the curve on freezing. This would ordinarily indicate damage. However, considering the low effective resistance values and a value of  $\phi_p = 0.110$ , damage is not expected to be significant.

The air-entrained samples that were resaturated with salt solutions did not fare as well as expected. It appears that the drying of the samples resulted in a coarsening of the pore structure that created more links to the air-entrainment. On resaturation, a portion of the air-entrainment became saturated. The effective freezing resistance (EFR) values are relatively high as well as their pore blocking temperatures. These values would indicate that these samples are susceptible to frost damage.

### 3. Thermo Mechanical Analysis

The length change of saturated porous materials was determined during the freezing-thawing cycle, Figure 8. The length change-temperature curves have been extensively studied and the characteristic features are described in detail elsewhere [4]. The uniqueness of the current study is that the length change data and electrical characteristics (impedance spectra) were determined on the same specimen during the freezing-thawing experiment. Pore water movement and ice formation during a freezing cycle can result in an expansion. Dilation (in this study) is defined as the difference in the relative length change of the specimen over the temperature range  $+20^{\circ}\text{C}$  to  $0^{\circ}\text{C}$  and the final relative length over the temperature range  $0^{\circ}\text{C}$  to  $-20^{\circ}\text{C}$ . The expansion (or dilation), hysteresis (on thawing) and residual length change are measures of the extent of frost damage and are typically large in a cement paste sample that has undergone significant damage (see Table 1).

### 4. Damage Assessment - Coupled TMA and ACIS

Damage of cement paste due to freezing-thawing cycles has been traditionally assessed by characteristics of the length change-temperature curve e.g. dilation during freezing and residual length change on thawing. The electrical methods offer an alternate means of assessing damage.

The two curves (resistance and  $\rho$  versus temperature) are very closely related. One event occurring within the sample will be indicated by a change in both curves. Resistance reflects the amount of pore water freezing within the sample whereas  $\rho$  represents the effect that freezing has on the effective pore size distribution. The evaluation of the information provided in both curves will give a good indication of the damage resulting from the freezing-thawing cycle. Interpreting the freezing-thawing behaviour of the sample from either curve independently may lead to misleading results. In general, a high initial resistance and small changes in the value of  $\rho$  on freezing are indicative of a fine uniform pore structure and a durable cement paste. The lower the value of the effective freezing resistance the more durable is the cement paste system. Further, hysteresis in the  $\rho$ -temperature curve on thawing can be indicative of damage.

The complete set of freezing-thawing test parameters (electrical measurements and thermal mechanical analysis) obtained in this study is given in Table 1.

The results generally correspond to well known behavior i.e. high water-cement ratio pastes are vulnerable to frost attack. The deleterious action of salt is also evident. Larger values of all the parameters are generally indicative of reduced frost resistance. The well-known beneficial effects of air-entrainment are evident. The significance of the electrical measurements was discussed in the previous section.

## 5. Model Porous Systems-Vycor Glass and Clay Brick

### (i) Vycor Glass

Vycor glass is a porous material that has been used to model the freezing behavior of hydrated cement paste. Vycor glass has a very narrow pore size distribution with a mean pore diameter of about 2.5 nm.

Resistance-temperature and  $\phi$ -temperature curves (freezing-thawing) were obtained for vycor glass samples saturated with synthetic pore solution, Figure 9. Changes in the slope of these curves occur in the temperature interval -10 to -30°C (in concurrence with the length change behavior observed in the TMA analysis). Freezing of pore solution occurs in this range. The steep slope of the resistance-temperature curve over a small temperature range indicates that freezing is occurring in a pore system comprised of pores of relatively uniform size. Once freezing begins it continues at the same rate until water in all the pores has frozen. The resistance and  $\phi$  versus temperature curves approach a constant value after freezing is complete. The  $\phi$  parameter reaches unity and resistance changes nominally with decreasing temperature. The resistance and  $\phi$  values for cement paste systems continue to increase even after the freezing of the pore water is apparently complete. This may be due to differences in orientation effects of water within the absorbed layer.

Another indication of the uniform pore structure of the vycor glass is the narrow range of the  $\phi$  values on freezing. The majority of specimens had an initial  $\phi$  value of approximately 0.9 with a total increase of  $<0.1$  on freezing. However on thawing, damage to the vycor glass specimens is likely because of the large  $\phi$  (at 5°C) after one freezing -thawing cycle. This value is as much as 0.3, which indicates a significant change (due to formation of cracks on freezing) in the properties of the specimen.

### (ii) Clay Brick

The pore structure of clay brick is significantly different than that of cement paste. High durability (re. freezing-thawing) has been linked to bricks with pores larger than 1-3  $\mu\text{m}$ . A large, open and continuous pore system (in brick) permits "drainage" to occur during the freezing process, indicative of frost resistance. This does not normally occur in cement paste containing large pores.

The impedance data for a specific Canadian brick (considered durable) subjected to a freezing-thawing cycle indicate small changes in  $\phi$  values on freezing to -40°C and thawing to +5°C ( $\leq 0.10$ ). These values in combination with large values of the effective freezing resistance (EFR) are compatible with field experience indicating good durability. The

freezing of the pore water is easily accommodated without a significant amount of damage to the pore structure.

Two other bricks considered less durable (based on Canadian experience) had larger  $\tan \delta$  values on freezing even though this was accompanied by smaller values of the effective freezing resistance. Water movement cannot be as easily accommodated in these bricks which contain more fine pores in a less well connected pore system. Resistance to the water movement creates larger  $\tan \delta$  values. This damages the pore structure (since the brick is relatively weak).

## CONCLUDING REMARKS

Impedance spectroscopy appears to be a promising technique for analyzing the behavior of cement systems subjected to freezing-thawing cycles. The impedance data reflect the amount of pore water freezing and the mobility of the pore water. Incipient freezing can be identified by the first change in the slope of the resistance-temperature curve. The effective freezing resistance (EFR) parameter correlates with the amount of pore water freezing. The movement of the pore water and the amount of the unfrozen water in the pores influence the shape of the  $\tan \delta$ -temperature curve and the magnitude of  $\tan \delta$ .

Analysis of the shape of the  $\tan \delta$ -temperature curve on freezing and thawing gives information on the pore size distribution of the cement paste. A large and open pore structure results in a shallow curve and high pore blocking temperature indicated by a minimum in the value of  $\tan \delta$ . Pore blocking due to ice nucleation inhibits electrical conductivity and is dependent on the characteristics of the pore system. Conversely a deep  $\tan \delta$ -temperature curve is indicative of a system of fine pores that will become blocked at a lower temperature. The extent of hysteresis (on freezing-thawing) in the  $\tan \delta$ -temperature curve corresponds to the degree of damage.

The analysis of the resistance and  $\tan \delta$  versus temperature curves for vycor glass and clay brick indicates the responses for these model systems are consistent with the arguments presented for the behavior of cement paste systems. Damage indicators based on thermo-mechanical analysis (dilation, residual length change) are consistent with indicators based on electrical measurements (effective freezing resistance (EFR) and changes in the depression angle parameter,  $\tan \delta$ ). It is suggested that electrical methods have promise as a basis for development of new rapid methods of durability testing and new test standards.

## ACKNOWLEDGEMENTS

The authors would like to thank Messrs. Bob Myers, Gary Polomark and Gordon Chan for their help with the experimental work.

## REFERENCES

1. G.G. Litvan, Phase transitions of absorbates IV. Mechanism of frost action in hardened cement paste", J. Amer. Ceram. Soc, 1972; 55 (1): 38-42.
2. T.C. Powers, Working hypotheses for further studies of frost resistance of concrete Proc. Amer. Concr. Inst., 1945; 16 (4): 245-72.
3. T.C. Powers and R.A. Helmuth, Theory of volume changes in hardened portland cement paste during freezing Highw. Res. Bd., Proc. Annu. Meet, 1953; 32, p. 285-297.
4. G.G. Litvan, Phase transitions of adsorbates, III, Heat effects and dimensional changes in non-equilibrium temperature cycles, J. Colloid, Interface Sci., 1972; 38 (1): 75-83.
5. D.H. Everett, The thermodynamics of frost damage to porous solids Trans. Faraday Soc., 1961; 57 (104): 1541-1551.
6. R.E. Feldman, Length change adsorption, relations for the water-porous glass system to  $-40^{\circ}\text{C}$ . Can. J. Chem, 1970; 48: 287-297.
7. G.W. Scherer, Crystallization in pores, Cem. Concr. Res., 1999; 29 (8): 1347-1358.
8. T.C. Powers, Basic considerations pertaining to freezing- and -thawing tests, Am. Soc. Test. Mater. Proc. 1955; 55: 1132-1155.
9. R.A. Olson, B.J. Christensen, R.T. Coverdale, S.J. Ford, G.M. Moss, H.M. Jennings, T.O. Mason and E.J. Garboczi, Interpretation of the Impedance Spectroscopy of Cement Paste via Computer Modelling, Part III Microstructural Analysis of Frozen Cement Paste, J. Mater. Sci. 1995; 30: 5078-5086.
10. O. Katsura and E. Kamada, A mechanism of frost damage of concrete under supercooling, in Frost Resistance of Concrete, Eds. M.J. Setzer and R. Aberg, EZFN Spon, London, 1997; p. 202-211.
11. P. Gu, P. Xie, Y. Fu and J.J. Beaudoin, Microstructural characterization of cementitious materials: conductivity and impedance methods, in Materials Science of Concrete IV, Eds. J. Skalny and S. Mindess, The American Ceramic Society, Westerville, Ohio, 1995, p. 201-262.
12. W.J. McCarter, S. Garvin and N. Bouzid, Impedance measurements on cement paste, J. Mater. Sci., Lett., 1988; 7 (10): 1056-1057.

13. C.A. Scuderi, T.O. Mason and H.M. Jennings, Impedance spectra of hydrating cement pastes, *J. Mater. Sci.*, 1991; 26: 349-354.
14. Z. Xu, P. Gu, P. Xie and J.J. Beaudoin, Application of a.c. impedance techniques in studies of porous cementitious materials, (II): Relationship between ACIS behaviour and the porous microstructure, *Cem. Concr. Res.*, 1993; 23 (4): 853-862.
15. J. Ross Macdonald, Editor, *Impedance spectroscopy*, J. Wiley & Sons, Toronto, 1987.
16. P. Gu, P. Xie, Y. Fu and J.J. Beaudoin, A.C. impedance phenomena in hydrating cement systems: frequency dispersion angle and pore size distribution, *Cem. Concr. Res.*, 1994; 24 (1): 86-88.



## FIGURE CAPTIONS

- Figure 1. (a) Schematic plot of a high frequency arc in the impedance complex plane obtained for cement paste systems. (b) A simplified electrical equivalent circuit for hydrating cement systems.  $R_1$ ,  $R_2$ , and  $C_2$  are high-frequency resistance, solid-liquid interface resistance and capacitance.  $R_{ct}$  and  $C_{dl}$  are cement-electrode interface charge transfer resistance and double layer capacitance.
- Figure 2. A pore size distribution curve for a durable Canadian clay brick sample.
- Figure 3. Impedance spectra (high frequency arc) of hydrated Cement Paste Obtained during a Freezing Cycle
- Figure 4. Typical Resistance versus Temperature curves for Cement Paste subjected to a Freezing cycle ( $w/c=0.60$ ).
- Figure 5 (a). The Effective Freezing Resistance (cement paste specimens) versus the Integral of the Heat Flow curve (determined by DSC).
- Figure 5 (b). The Resistance Ratio,  $R/R_0$ , on cooling versus Temperature.
- Figure 6. A typical  $\Delta R$ -Temperature curve for a Cement Paste. The Resistance-Temperature curve is super imposed on the  $\Delta R$ -T curve, ( $w/c=0.60$ ; 1d).
- Figure 7. Four types of  $\Delta R$ -Temperature curves for Cement Paste subjected to a freezing-thawing cycle. Type 1 - Paste at early age; Type 2 - Paste containing Salt solutions; Type 3 - Air-entrained paste; Type 4 - Paste at advanced ages of hydration.
- Figure 8. Typical Length Change Isosteres for Cement Paste ( $w/c=0.60$ ).
- Figure 9. Resistance and  $\Delta R$  versus Temperature curves for Vycor Glass.

Table 1 - Freezing-Thawing Test Parameters

Sample	Pore Blocking Temp (PBT) (°C)	? ? PBT	? ? Cycle	Dilation (μm/m/°C)	Residual Expansion (μm /m)	Effective Freezing Resistance	Heat Flow (J/g)	
Cement Paste w/c=0.35								
Age	1 Day	-16	0.06	-0.038	157	2230	75	27.98
	3 Days	-25	0.05	-0.004	135	300	21	19.15
	7 Days	-28	0.06	-0.008	80	250	15	10.18
	28 Days			-0.022	50	-1000		4.93
w/c=0.35 10% Salt Soln								
Age	7 Days	-28	0.24	0.116	125	550	27	17.80
	28 Days	-23	0.03	0.026	225	-3000	22	22.08
w/c=0.60								
Age	1 Day	-13	0.10		309	2207	1080	
	7 Days	-26	0.06	-0.033	234	1200	28	17.59
	28 Days	-26	0.10	-0.041	104	2100	18	
w/c=0.60 10% Salt Solu								
Age	7 Days	-26	0.37	0.695	223	1000	400	51.47
	28 Days	-25	0.29	0.353	208	500	227	52.30
w/c=0.35 6% Air								
Age	7 Days	-37	0.27	0.057	-13		9	16.20
	28 Days	-39	0.18	0.110	-20		7	4.80
	28Days (10% salt sol)	-15	0.04	0.047	2		5	8.80
w/c=0.60 6% Air								
Age	28 Days	-16	0.18	0.023	240	1076	10	

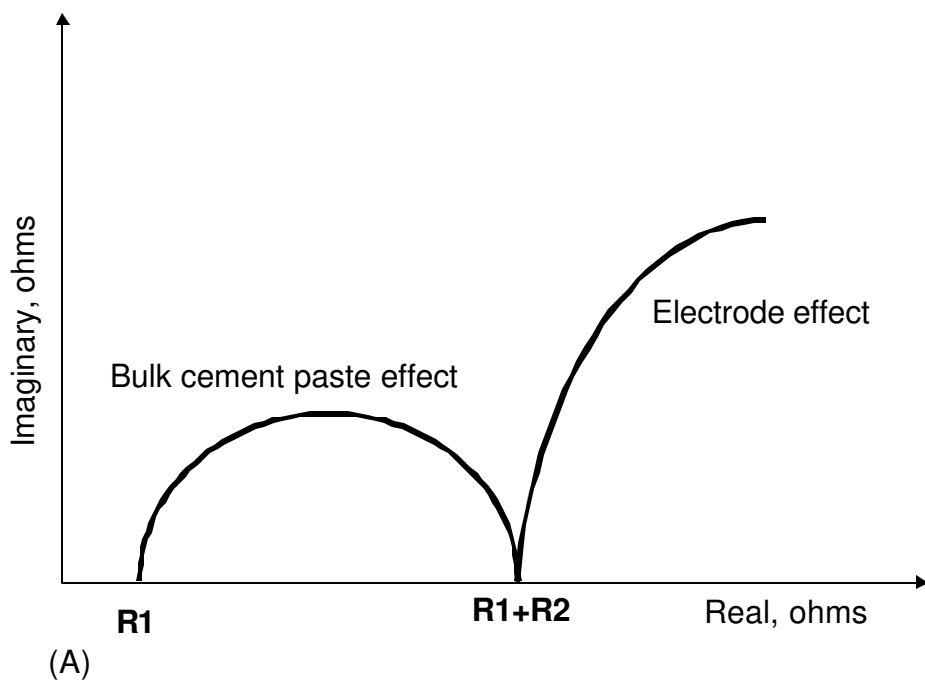


Figure 1a

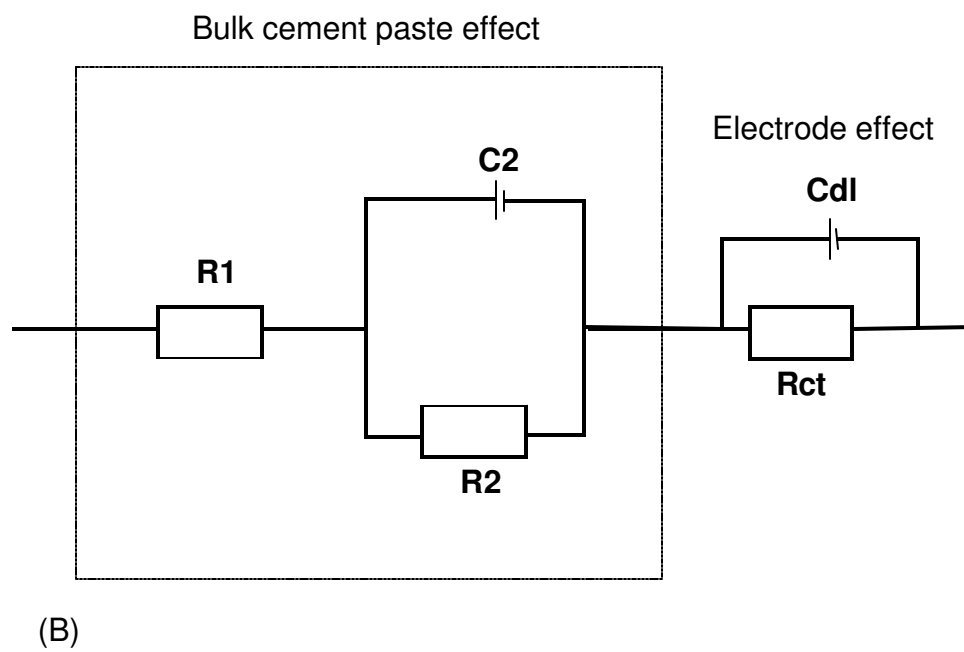


Figure 1b

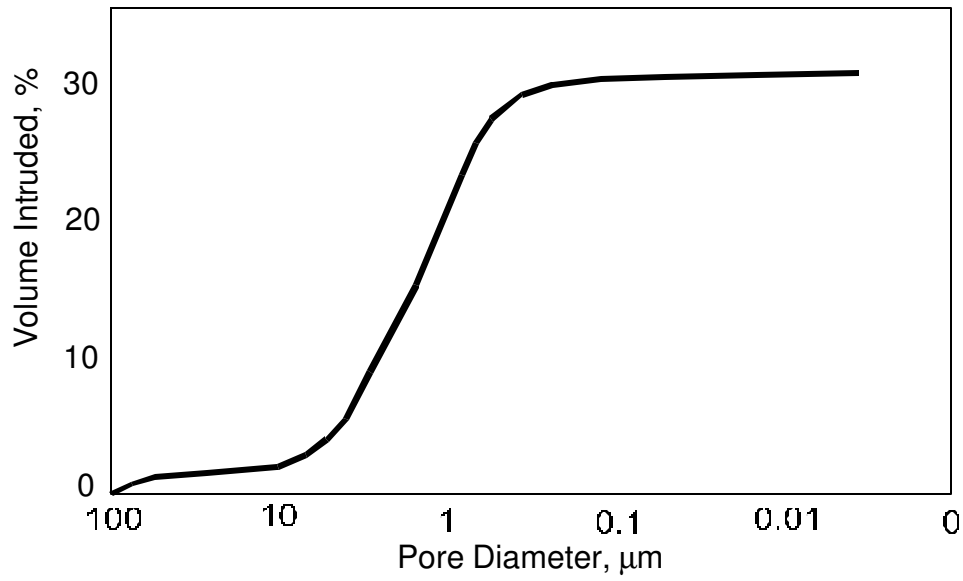


Figure 2

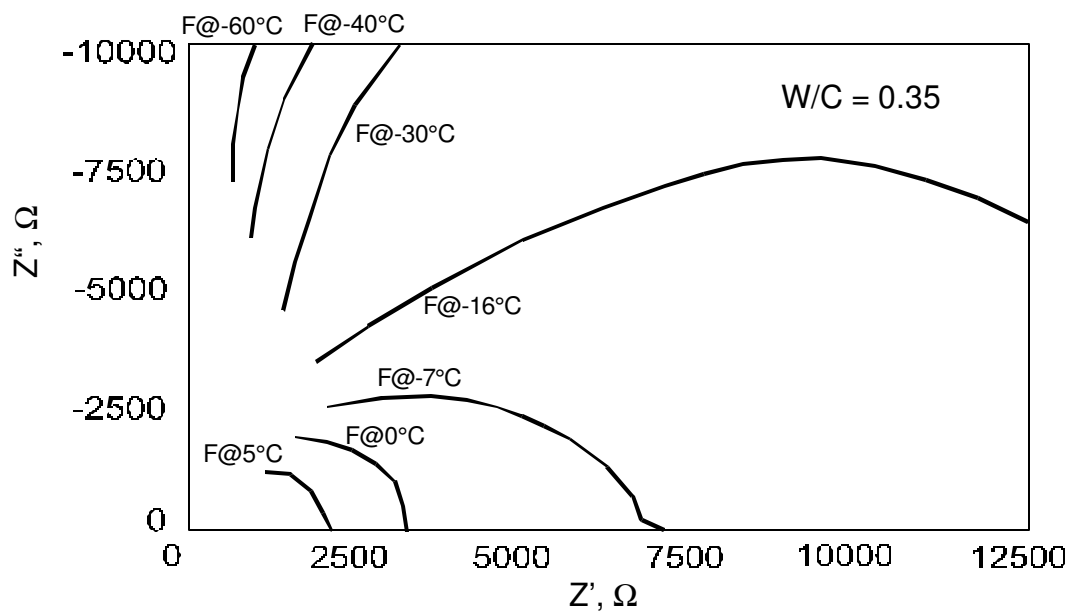


Figure 3

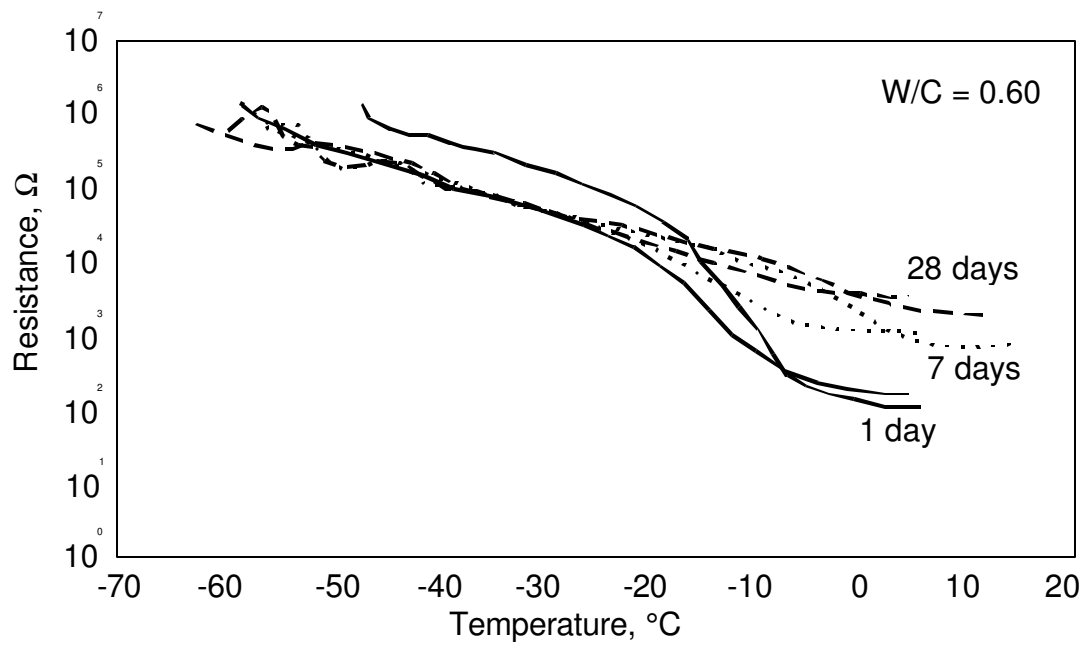


Figure 4

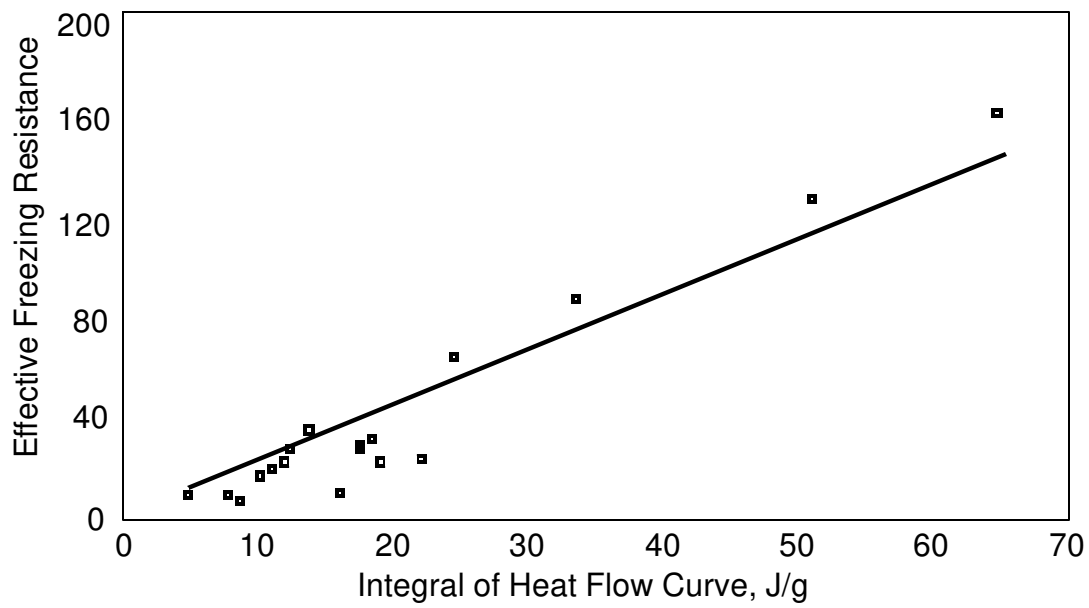


Figure 5a

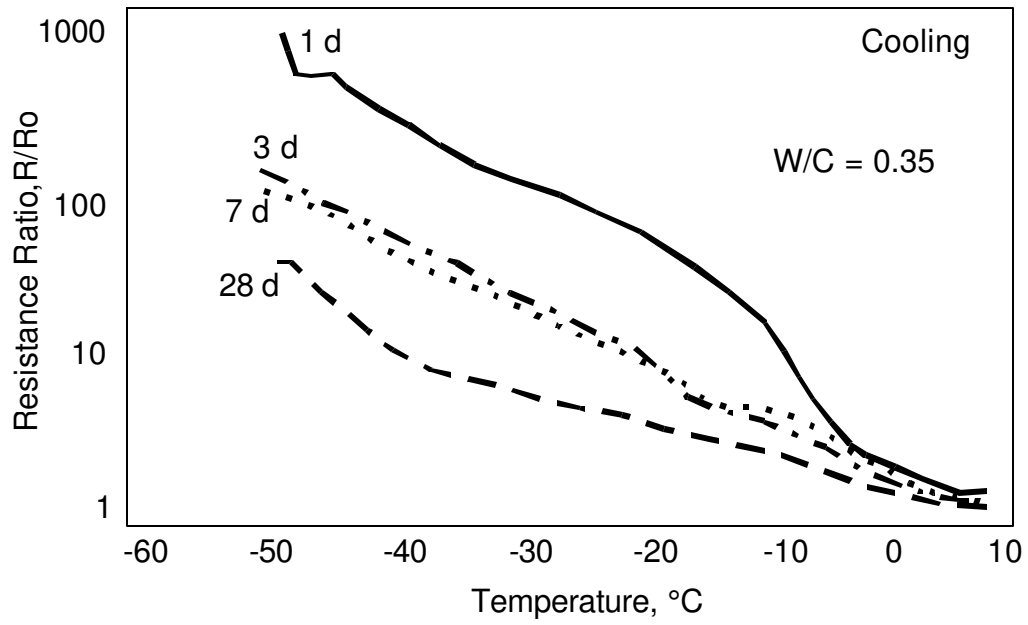


Figure 5b

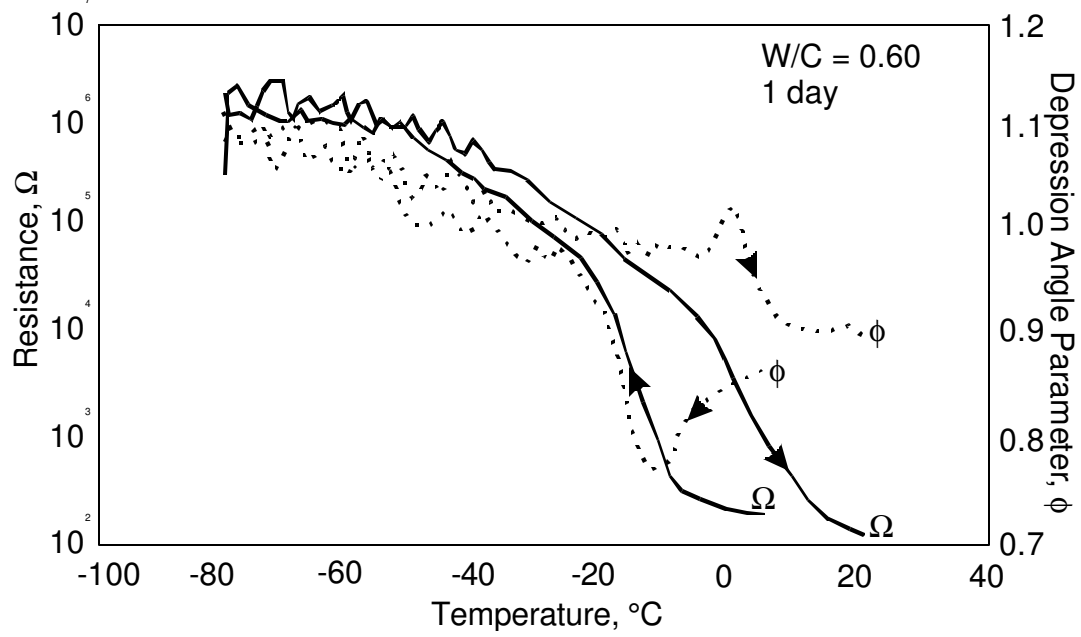


Figure 6

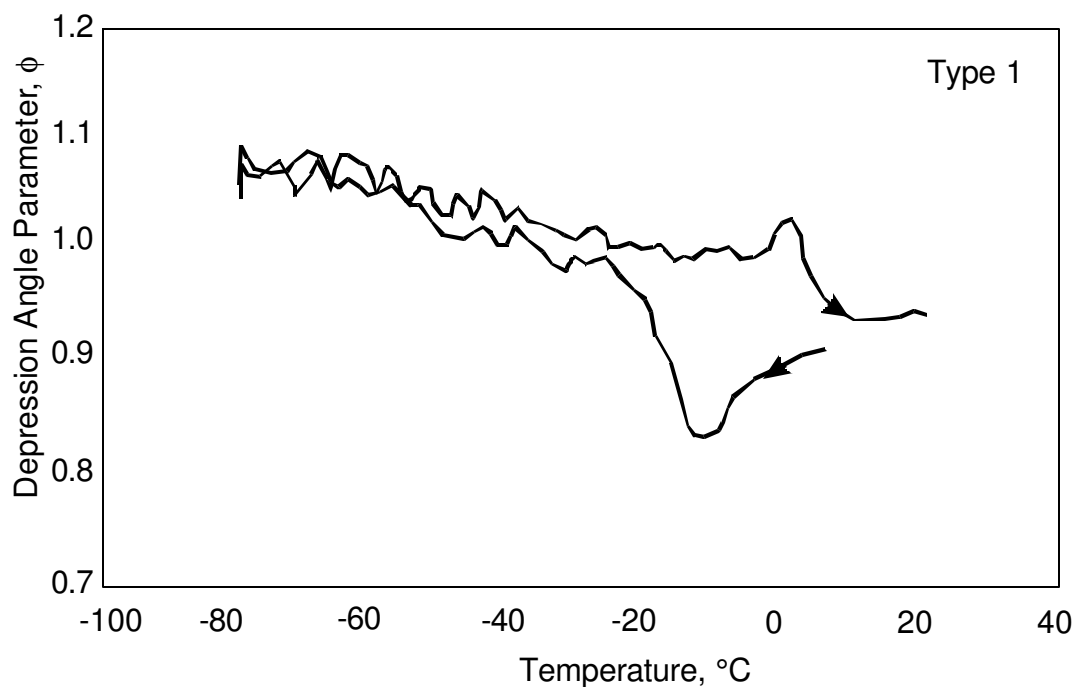


Figure 7a

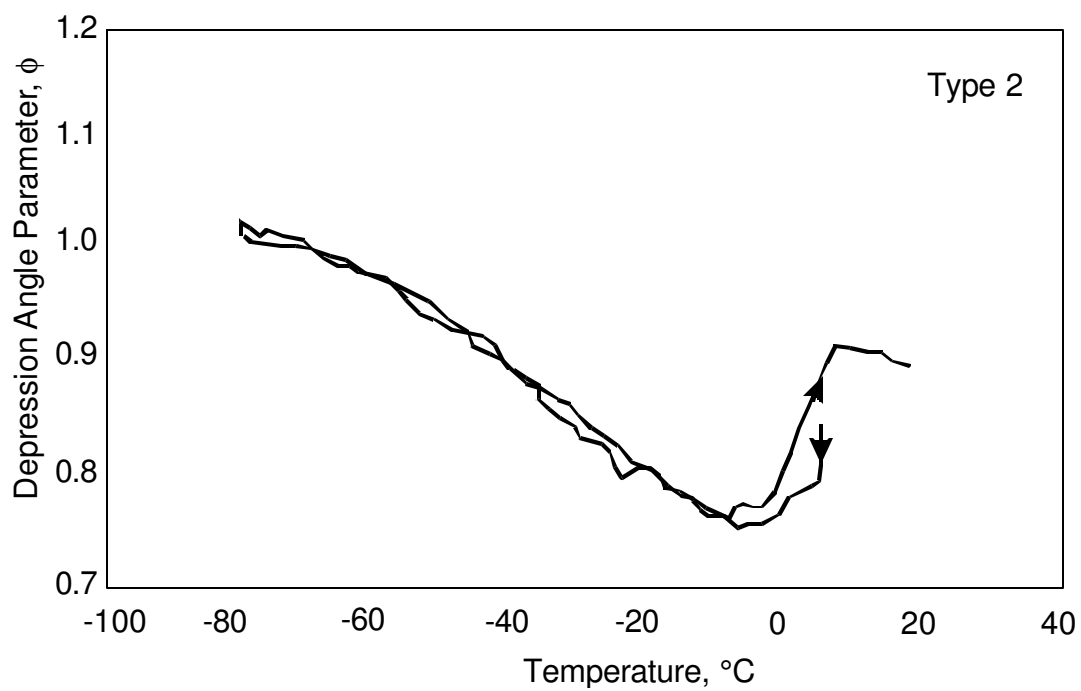


Figure 7b

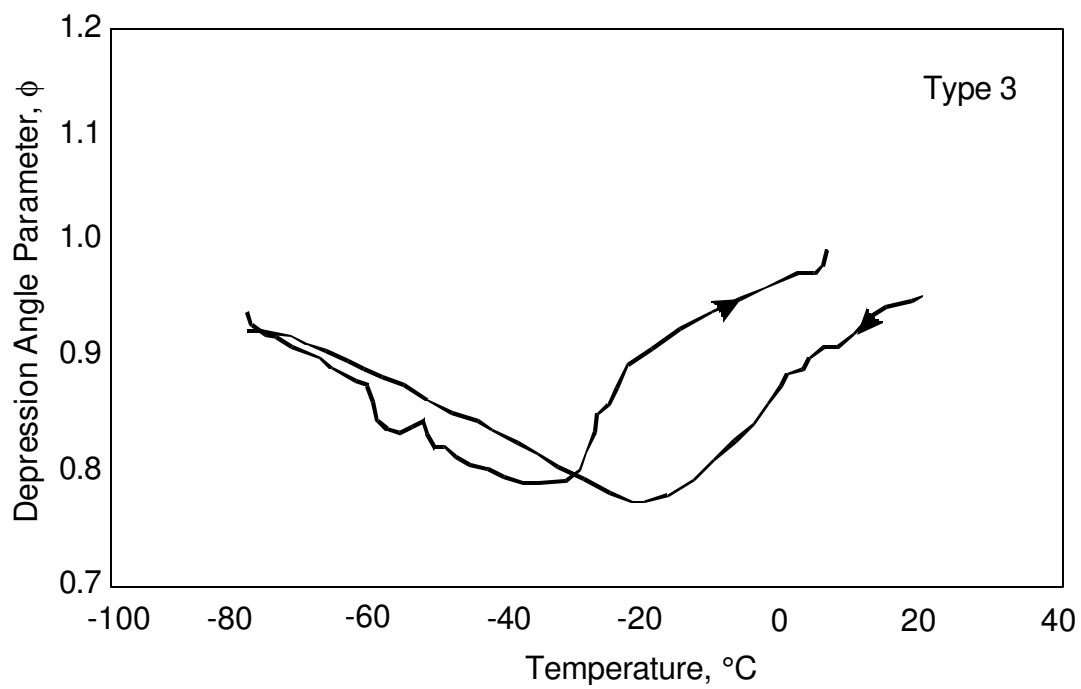


Figure 7c

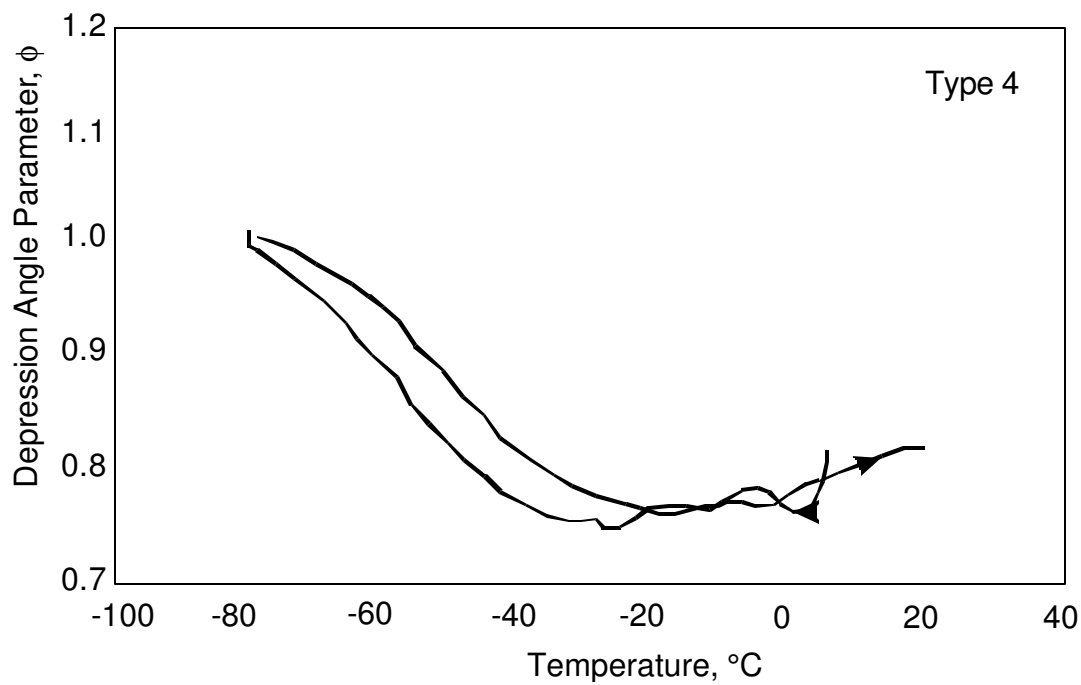


Figure 7d



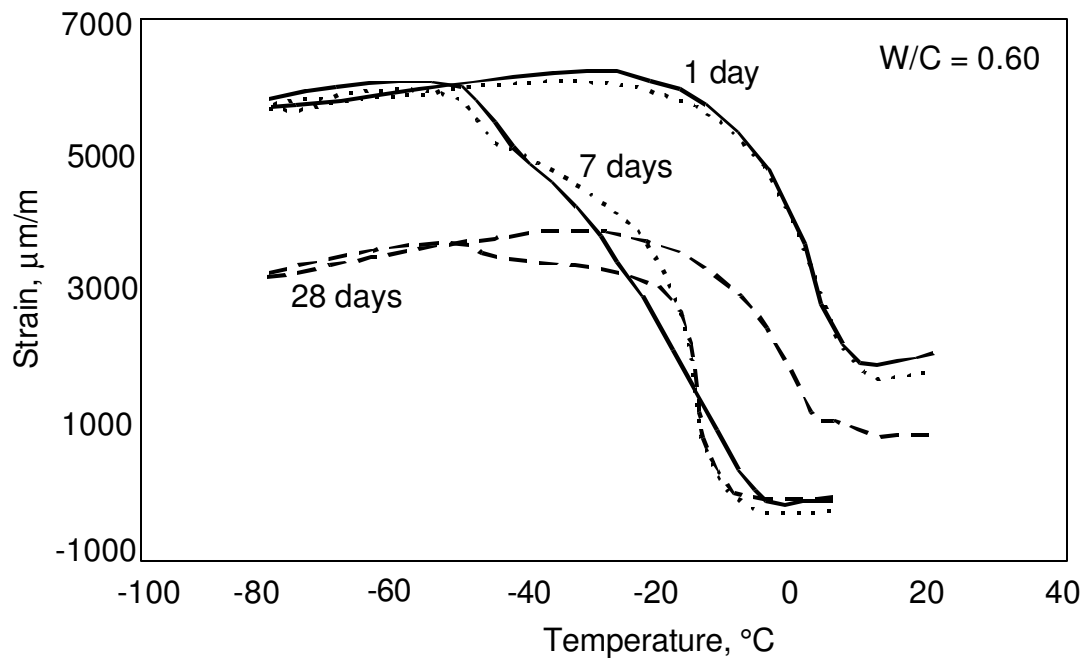


Figure 8

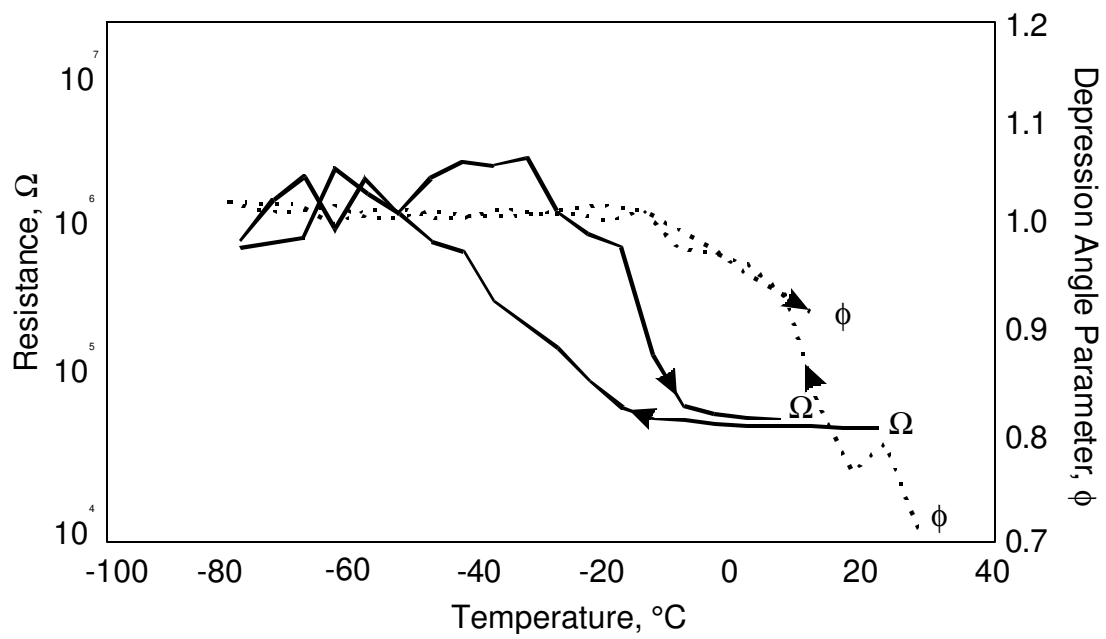


Figure 9